

## Analysis of End-Point with Power Consumption in High Speed Mixer

Keijiro TERASHITA,<sup>\*,a</sup> Masaya KATO,<sup>a</sup> Atsuo OHIKE,<sup>b</sup> and Kei MIYANAMI<sup>a</sup>

Department of Chemical Engineering, University of Osaka Prefecture,<sup>a</sup> Mozu-Umemachi, Sakai, Osaka 591, Japan and Technological Development Laboratories, Fujisawa Pharmaceutical Co., Ltd.,<sup>b</sup> Kashima, Yodogawa-ku, Osaka 532, Japan. Received November 17, 1989

A granulation experiment was conducted using different granulator and formulation. The purpose of the experiment was to clarify the granulation end-point to gain high yields of spherical, well-compacted granules and fine granules, and to investigate the agitation-granulating process. The fluctuation of electric-power consumption was continuously measured during the granulation operation, and it was determined that measurement of power consumption was helpful for determining the granulation process and granulation end point.

One of the results of the experiment was that the granulation process was divided into four phases, and at the initial stage of phase IV high yields of spherical, well-compacted granules and fine granules are possibly produced (granulation end-point). It was found that the granulating mechanism in each of the phases is not affected by the use of different agitation granulators, formulations, or the binder addition time adopted. The specific binder addition time and granulator model that produced high yields of granules and fine granules were identified.

**Keywords** granulation end-point; power consumption; granulation mechanism granules; fine granules; high speed type mixer

### Introduction

Recently "good manufacturing practice" has been an indispensable element in the pharmaceutical industry. In addition, active attempts at factory automation have been required to meet the pressing needs to control the quality of pharmaceutical formulations. To ensure full factory automation for the production of solid dosage forms, the measurement and control of individual unit operations on the production line must be established. This automation requires the manipulation of individual-unit apparatus guided by sensors, to eliminate human error and to secure production of uniform quality products.

We focused our attention on the agitation granulation process, which plays an important role in the production of solid dosage forms. To offer a new perspective for office equipment, we reported on a method to determine the granulation end-point using the power consumption curve.<sup>1-3)</sup> The granulation end-point is the point at which high yields of spherical, well-compacted granules and fine granules are produced. Other researchers<sup>4-6)</sup> have reported on the possibilities of determining the granulation end-point using a measurement of power consumption (agitation torque). We believe, however, the granulation end-point should be determined after a thorough examination of the granulation process, including the use of different granulator models and models of formulation.

We therefore conducted experiments with different agitation granulator models, binder addition times, and formulations, so as to verify the method of determining the granulation end-point by measurements of power consumption. In addition, the shapes and properties of the granules were observed, and the yields corresponding to different power consumption levels were investigated. As a result, the granulation process was divided into four phases and the granulation mechanism in each phase was examined. Next, the granulation end-point at which high yields of spherical and well-compacted granules and fine granules are produced was determined. This determination leads to an indication of the appropriate binder addition time and granulator model.

### Experimental

**Powder Samples and Binder** The powder samples used for the experiment were the same as previously reported<sup>1-3)</sup> shown in Table I. With the exception of sucrose, which was hammer-milled, powder samples were bought from the general market. We used purified water for the binder.

**Apparatus and Method** A high speed mixer (10-liter capacity) and a versatile mixer (5-liter capacity) which is a kind of planetary mixer, of the same type as previously reported,<sup>1-3)</sup> were used. Both were commercially available. The power consumption of the agitator and chopper were automatically measured while the product temperature was being displayed (Fig. 1).

The power consumption of the versatile mixer was continuously recorded, as previously reported. A standard power sensor was used during

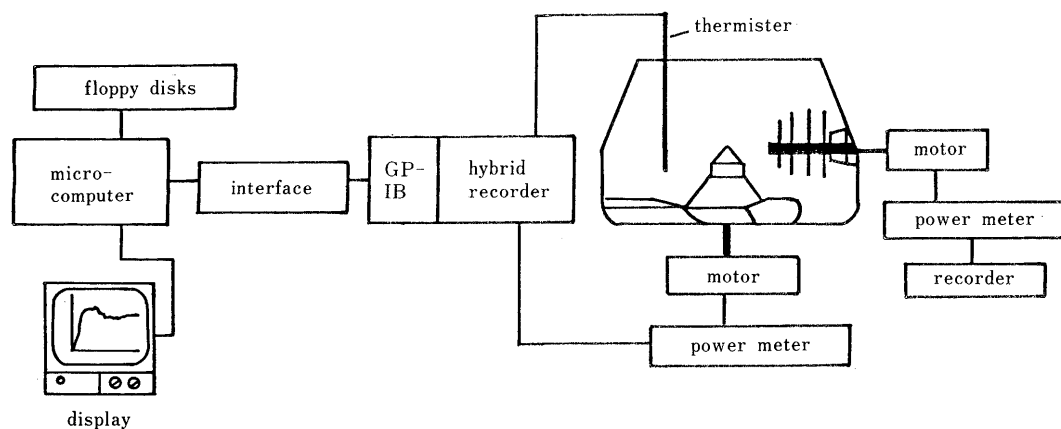


Fig. 1. Apparatus and Monitoring System of Power Consumption and Object Temperature

TABLE I. Powder of Sample

Sample	Particle diameter ( $\mu\text{m}$ )	Density ( $\text{kg}/\text{m}^3$ )	Apparent density ( $\text{kg}/\text{m}^3$ )	Angle of repose (rad)
Lactose	74	1430	458	0.773
Sucrose	20	1440	366	0.867
Corn starch	15	1330	354	0.991
Crystalline cellulose	40	1370	321	0.768

the experiment. Triple blades were used for agitation in the high speed mixer. The versatile mixer<sup>1</sup> used a single-screw beater for granulation. For the agitation/granulation we used lactose or sucrose, corn starch, and crystalline cellulose in powder form compounded in the ratio of 6:3:1 by weight. The weight of the powder samples fed into the mixers was 2.5 kg for the high speed mixer and 1.0 kg for the versatile mixer.

The granulation experiment was conducted as previously reported.<sup>1-3</sup> First, the weighed powder samples were fed into the mixer and agitated for about 180 s to ensure the appropriate amount of mixing and packing of the powder samples. Next, the agitator blades were run at different rps's, while the binder was added from the top of the agitation vessel. The lactose/corn starch/crystalline cellulose mixture (hereinafter referred to as "formulation I") was granulated either by adding the binder all at once or by varying the adding time. The binder addition time was adjustable by changing the revolution speed of the roller pump.

The sucrose/corn starch/crystalline cellulose compound (hereinafter referred to as "formulation II") was only added all at once. Formulation I was intended for producing granules while formulation II was intended for producing fine granules. The high speed mixer was used at an agitator speed of 8.3 revolution/s and a chopper speed of 50.0 revolution/s. The versatile mixer was used at a blade speed of 2.10 revolution/s and 6.30 rotation/s for granulation.

**Evaluation of Granule Properties** The granules were ventilation-dried (on a shelf) at 318 K (45 °C) for 12 h. The particle-size distribution was determined by sieve analysis with a rotating sieve shaker. Shape index, and apparent density of the granules and fine granules were measured in the same manner as previously reported.<sup>2</sup> The current discussion will therefore be brief. The particle-size distribution, shape index, and apparent density ( $\rho_a$ ) were measured by screening, a short/long diameter ratio, and a graduated cylinder, respectively. Granule yield  $Y_G$  and fine granule yield  $Y_S$  were calculated by dividing the granule (12–48 mesh) yield and fine granule (32–150 mesh) yield, respectively, by the total-granule yield.

## Results and Discussion

**Granulation Process and Granulation End-Point** It was previously reported<sup>1-3</sup> that identification of the granulation end-point for the granulation process in a mixer-granulator is possible by measuring power consumption. Accordingly, this experiment was intended to determine the granulation end-point that produced the highest yields of well-compacted, spherical granules and small particles. This was done by observing the granulation process in relation to the power consumption level. An example of the measured values of the agitator and chopper-power consumption  $P$  and temperature  $\Delta T_e$  (difference between object temperature and initial temperature) is shown in Fig. 2.

The powder sample was the lactose/corn starch/crystalline cellulose compound (formulation I). The binder was added at the rate of  $W_B = 21$  wt.% at the same time as the powder sample. Figure 2 shows, as previously reported,<sup>3</sup> that the granulation process has different phases related to the power consumption  $P$  (shown as a solid line). In phase I,  $P$  grows. In phase II,  $P$  fluctuates. In phase III,  $P$  declines and in phase IV,  $P$  displays a constant  $P_S$ . Such categorization into four phases also applies to formulation II (sucrose/corn

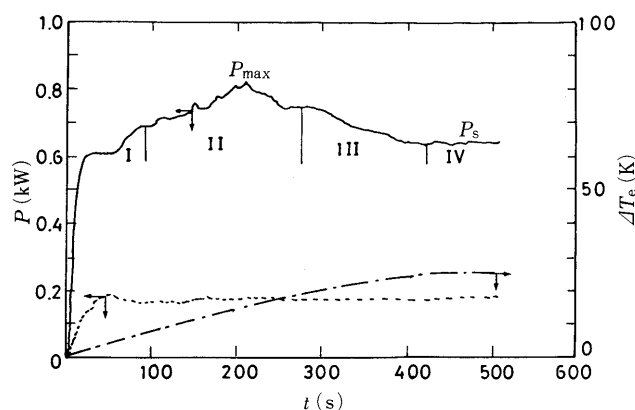


Fig. 2. Measurement of Power Consumption,  $P$ , and Temperature,  $\Delta T_e$ . High speed mixer; formulation I; binder addition ratio,  $W_B = 21$  wt.%; —, power consumption of agitator; - - - -, power consumption of chopper; - · - ·, temperature.

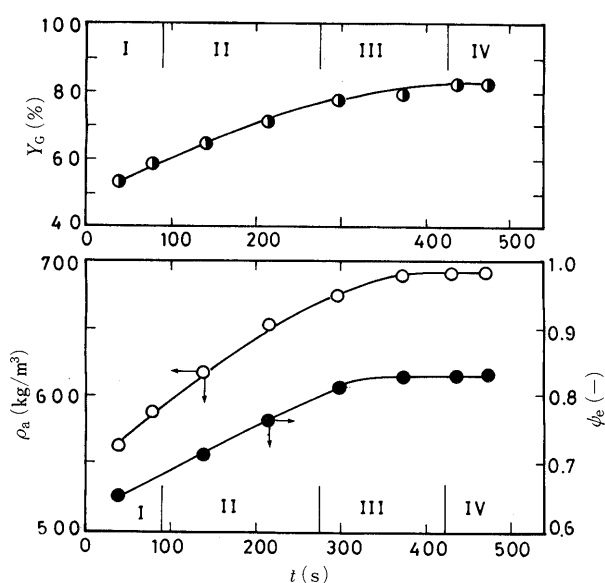


Fig. 3. Relationship between Granule-Yield,  $Y_G$ , Granule Apparent-Density,  $\rho_a$ , Shape Index,  $\psi_e$ , and Granulation Time,  $t$

High speed mixer; formulation I; binder addition ratio,  $W_B = 21$  wt.%; ○, granule-yield; ○, granule apparent-density; ●, shape index.

starch/crystalline cellulose).<sup>3</sup> This is the same categorization used in the previous report. Temperature  $\Delta T_e$  indicates a constant value during the initial stage of phase IV. This implies that using the power-consumption level to determine the granulation process is valid regardless of the formulation applied.

Figure 3 shows the relationship between the granule apparent-density  $\rho_a$ , the shape index  $\psi_e$ , and granulation time,  $t$ . The granule-yield  $Y_G$  and  $t$  are displayed, as well. I—IV represent each phase at different-power consumption levels.

Figure 3 shows that  $Y_G$ ,  $\rho_a$ , and  $\psi_e$  grows along with granulation time (phases I—IV). The constant value in phase IV implies that the granulation end-point, which produces high yields of well-compacted, spherical granules, exists during the initial stage of phase IV. The same principle applies to the study of the versatile mixer with formulation I.<sup>1,2</sup>

Figure 4 shows the power consumption levels that were obtained during the production of granules by the versatile

mixer and formulation II. It also shows the results<sup>3)</sup> from the high speed mixer. The granulating process using the versatile mixer was divided into four phases based on power consumption. The results are similar to those obtained with the high speed mixer. The maximum-power consumption  $P_{max}$  by the versatile mixer was obviously in phase II. This is probably caused by large agglomerates formed between the period of phase I and the initial stage of phase II.

Figure 5 shows an example of granules, observed under a scanning electron microscope, obtained in each of the phases described in Fig. 4. In phase I, nucleic granules are formed by the liquid-bridge action between granules caused by the addition of binder. In this phase many agglomerates are also found. By the shearing, rotation, and compaction of the blades (screw beater), well-compacted, spherical, fine granules are obtained during the transition from phase II to phase IV. In phase IV the fine granule yield is particularly high. This is also true when the high speed mixer is used.

From these studies, it became clear that the high-yield of well-compacted, spherical granules and fine granules during the initial stage of phase IV occurred regardless of the granulator model. Phase I: formation of agglomerates and nucleic granules; phase II: growth into granules; phase III: granular refinement; phase IV: final granulation process.

**Granulation Process and the Relationship between Granule Properties and Binder Addition Time** The relationship be-

tween the granulation process, power consumption levels, and binder addition time was observed and granule properties and granule-yield  $Y_G$  were measured. High-granule yield with the high speed mixer in formulation I was obtained at binder addition ratio  $W_B = 21$  wt. %.

Figure 6 shows an example of the agitator's power consumption corresponding to granulation actions for different binder addition times. The arrow in the figure shows the point at which the binder was completely added. Figure 6 clearly displays the results of changes in binder addition time. Accordingly, no further comment is made here.

Although variations in binder addition time  $t_e$  did not greatly effect phase II to IV, significant differences naturally

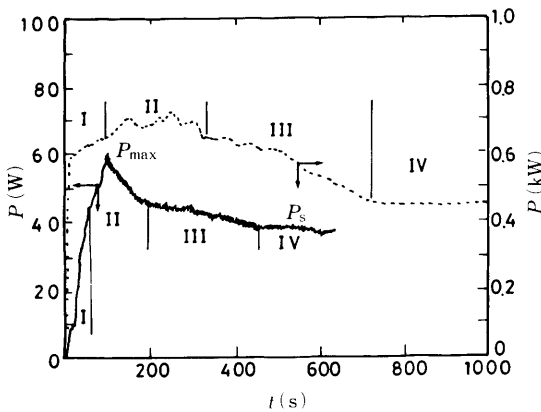


Fig. 4. Relationship between Power Consumption,  $P$ , and Granulation Time,  $t$

-----, high speed mixer; formulation II; binder addition ratio,  $W_B = 9.1$  wt.%;  
 —, versatile mixer; formulation II; binder addition ratio,  $W_B = 10.3$  wt. %.

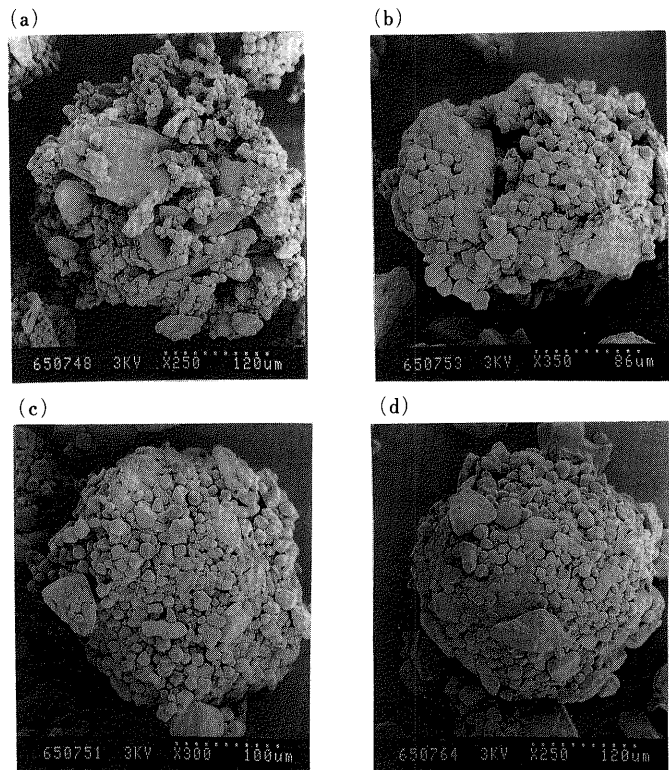


Fig. 5. Example of Granules Observed by a Scanning Electron Microscope

Versatile mixer; formulation II; binder addition ratio,  $W_B = 10.3$  wt.%. (a) phase I; (b) phase II; (c) phase III; (d) phase IV.

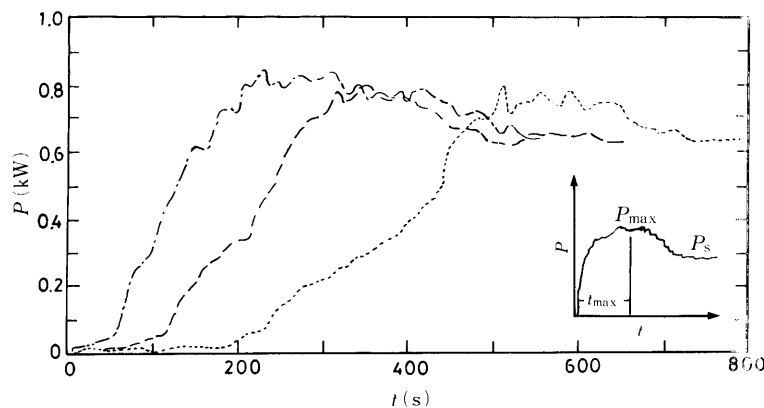


Fig. 6. Agitator's Power Consumption Obtained by the Change of Binder Addition Time,  $t_a$

High speed mixer; formulation I; binder addition ratio,  $W_B = 21$  wt.%; —,  $t_a = 160$  s; ---,  $t_a = 270$  s; ·····,  $t_a = 500$  s.

occurred in phase I. When the addition-time  $t_a$  is short, power consumption rises rapidly and the length of phase I is shortened. When the addition time is long, power consumption linearly rises lengthening phase I. These results indicate that when the addition time is short, agglomerates and nucleic granules are formed that remain in phase II. This situation is similar to adding all the binder at once resulting in insufficient dispersion of the binder. On the other hand, a longer addition period allows sufficient dispersion of the binder while a liquid bridge is gradually formed, causing the predominant formulation of nucleic granules rather than agglomerates. The lengthening of phase I accompanying increased binder addition time has been proved by an experiment employing a versatile mixer.<sup>2)</sup> Figure 6 shows that power consumption  $P$  indicates a constant value in phase IV for any given binder addition time  $t_a$  accordingly, and phase IV was identified as containing the granulation end-point, where the granulating operating ceased.

Next, a report will be made about the granules produced during the initial stage of phase IV. Figure 7 shows the 50% mean particle diameter  $D_{50}$  and the geometric standard deviation  $\sigma_g$  of granules produced with different binder-addition times  $t_a$ .  $D_{50}$  seems to indicate a gentle decrease with the increase of adding time.  $\sigma_g$  indicates a minimum value at  $t_a \approx 250$  s, where longer addition times indicated

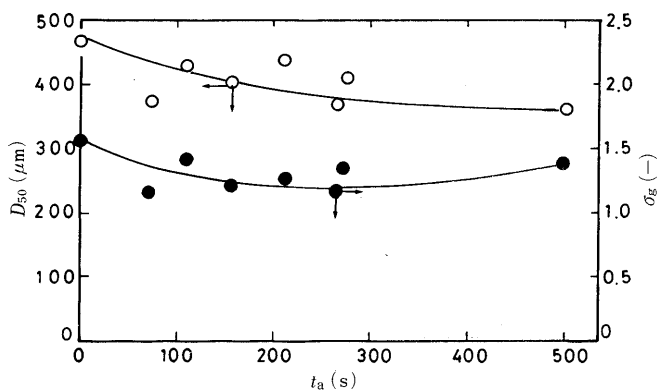


Fig. 7. Relationship between the 50% Mean Particle Diameter,  $D_{50}$ , the Geometric Standard Deviation,  $\sigma_g$ , and Binder Addition Time,  $t_a$ . High speed mixer; formulation I; binder addition ratio,  $W_B=21$  wt.%;  $\circ$ , 50% mean particle diameter;  $\bullet$ , geometric standard deviation.

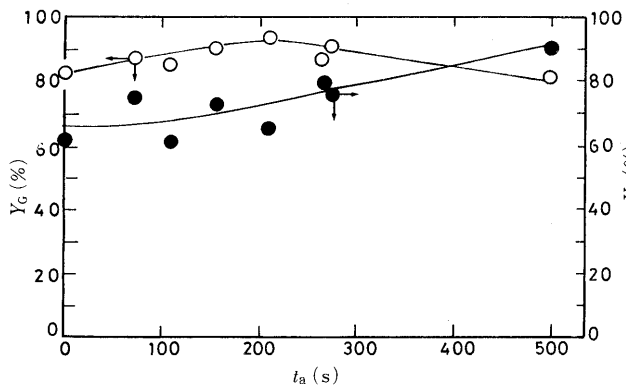


Fig. 8. Relationship between Granule-Yields,  $Y_G$ , and Binder Addition Time,  $t_a$ . High speed mixer; formulation I; binder addition ratio,  $W_B=21$  wt.%;  $\circ$ , granule-yield;  $\bullet$ , fine granule yield.

larger values.

Trends toward a smaller mean particle diameter and wider particle size distribution were also observed with granulating experiments using the versatile mixer.<sup>2)</sup> The causes of such granulation-process results are presumed to be as follows. A single addition ( $t_a=0$ ), which consumes very little time, causes insufficient dispersion of the binder during the initial stages of the granulation process (phase I). This causes many agglomerates to form, which are sheared and crushed into fine granules by the agitator and chopper. The agglomerates then adhere and promote granulation, yielding a large 50% mean-particle diameter. The nucleic particles formed in phase I develop into granules. Because there are two different patterns for the granulation process—(1) agglomerate/fine granules/granules and (2) nucleic particles/granules—the particle size distribution is wide ( $\sigma_g$  is large). In constant, with longer addition times, as mentioned before, nucleic-particle formation predominates, and these develop into granules. Therefore,  $D_{50}$  is comparatively small while granules with a uniform particle size distribution are produced. The small  $D_{50}$  and large  $\sigma_g$  for  $t_a=500$  s, are caused by moderate progress in nucleic-particle formation and granule generation. This implies that with long adding times, nucleic particles are crushed by the high-speed revolution of the agitator and chopper, inhibiting their granulation.

Figure 8 shows the relationship between granule-yield  $Y_G$  and binder addition time  $t_a$ . Fine granule yield  $Y_S$  is included as a reference. The highest granule yield was obtained with an addition time of  $t_a=180-280$  s. Larger  $t_a$  reduced  $Y_G$ . The reduced  $Y_G$  at  $t_a=500$  s is presumably because of the reduced mean-particle diameter  $D_{50}$ , implying a larger fine granule yield  $Y_S$ . Granule-yield  $Y_G$ , using the versatile mixer, and differentiated adding times were optimal at  $t_a=190-300$  s. It was somewhat lower at  $t_a=480$  s. A larger  $t_a$ , radically-degraded  $Y_G$ ,<sup>2)</sup> implies that higher granule yields are obtained at  $t_a=200-300$  s, regardless of the granulator model.

Figure 9 shows the relationship between the granular apparent density  $\rho_a$ , shape index  $\psi_e$ , and the binder addition time  $t_a$ . A granule-diameter range of 32–42 mesh was applied during the measurement of  $\rho_a$  and  $\psi_e$  to exclude the influence of particle-size distribution as much as possible in determining the two values. Figure 9 indicates that the

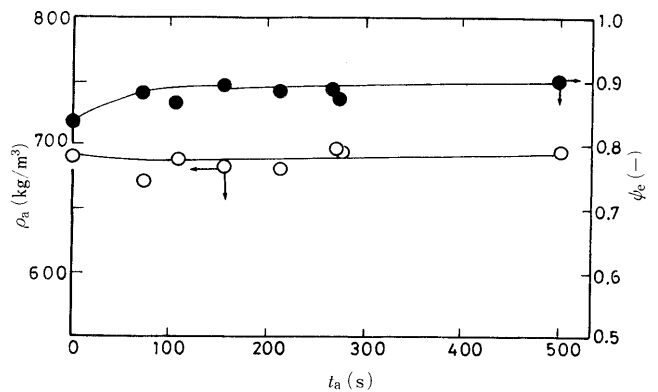


Fig. 9. Relationship between Granule Apparent-Density,  $\rho_a$ , Shape Index,  $\psi_e$ , and Binder Addition Time,  $t_a$ . High speed mixer; formulation I; binder addition ratio,  $W_B=21$  wt.%;  $\circ$ , granule apparent-density;  $\bullet$ , shape index.

granule shape index  $\psi_e$  is somewhat smaller for a single addition time while similar values are indicated for larger  $t_a$ ,  $\rho_a$  is only slightly affected by  $t_a$ . This implies that there is no substantial influence by  $t_a$  on this formulation for spherical shaping and compactness of granules.

The above results imply that binder addition time affects the particle-size distribution rather than the spherical shaping and compactness of granules. A higher granular yield is obtainable by compressing the particle size distribution. This compression is possible by setting the adding time at a little longer than one dispensing cycle. This can be done with the high-speed mixer-agitator and

versatile mixer.

**Comparison of Granules Obtained by High Speed Mixer and Versatile Mixer** Figure 10 shows the granule-yield  $Y_G$  obtained by differentiated binder addition  $W_B$  using the high speed mixer and the versatile mixer. The  $Y_G$  represents the initial stage of phase IV (granulation end-point). All the binder was added at one time. Figure 10 shows that a

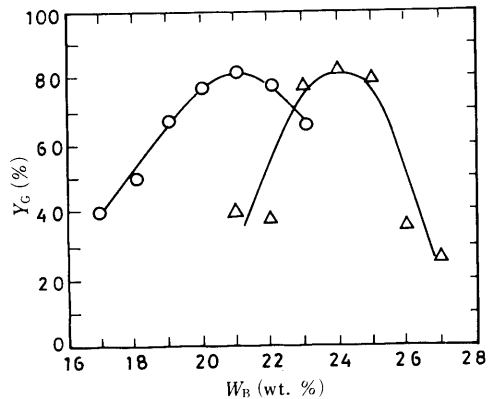


Fig. 10. Relationship between Granule-Yield,  $Y_G$ , and Binder Addition Ratio,  $W_B$

Formulation I; O, high speed mixer; Δ, versatile mixer.

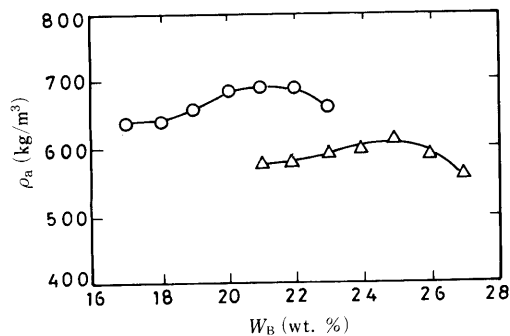


Fig. 11. Relationship between Granule Apparent-Density,  $\rho_a$ , and Binder Addition Ratio,  $W_B$

Formulation I; O, high speed mixer; Δ, versatile mixer.

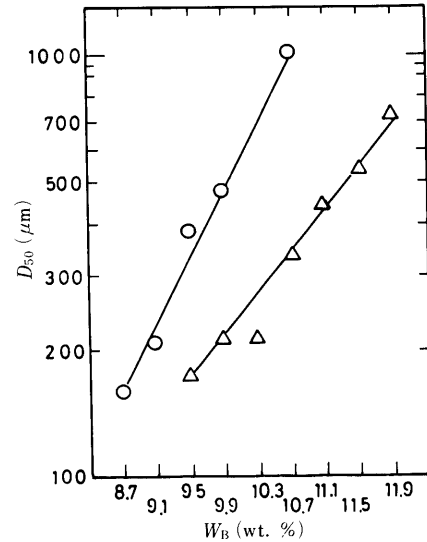


Fig. 12. Relationship between 50% Mean Particle-Diameter,  $D_{50}$ , and Binder Addition Ratio,  $W_B$

Formulation II; O, high speed mixer; Δ, versatile mixer.

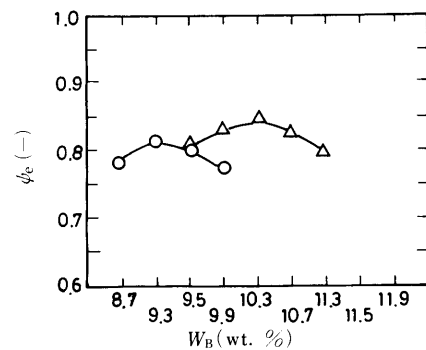


Fig. 13. Relationship between Shape Index,  $\psi_e$ , and Binder Addition Ratio,  $W_B$

Formulation II; O, high speed mixer; Δ, versatile mixer.

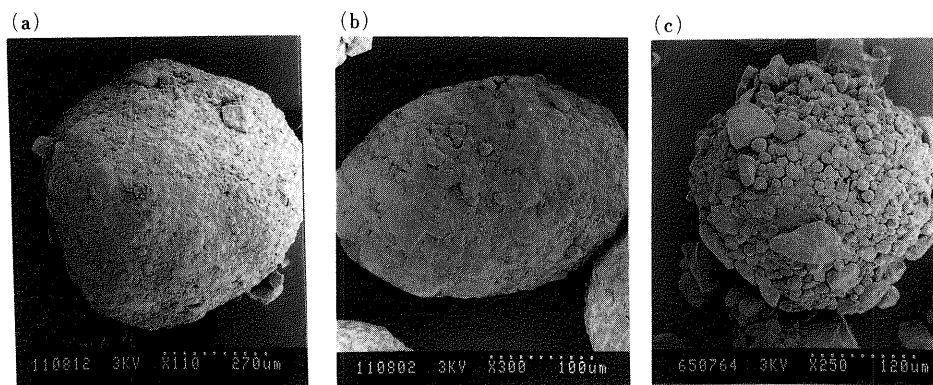


Fig. 14. Example of Granules Observed by a Scanning Electron Microscope

Formulation II; (a), (b) high speed mixer, binder addition ratio  $W_B = 9.1$  wt.%; (c) versatile mixer, binder addition ratio  $W_B = 10.3$  wt.%.

higher yield is obtained with the addition of less binder using the high speed mixer. This is attributed to the efficient liquid-bridge formation with less binder because of the effective dispersion of the binder by the action of agitator and chopper.

Figure 11 shows the apparent density  $\rho_a$  of granules obtained by the two models of the mixer-granulator. Granules of larger apparent gravity  $\rho_a$  and good contraction are obtained by using the high speed mixer. This yield is attributed to the significant effects of rotation and contraction created by the vortex circulation of the agitator. Figures 10 and 11 show that well-compacted granules are produced near the binder  $W_B$ , which produces a higher yield of granules.

Figure 12 shows the relationship between the 50% mean particle-diameter  $D_{50}$  and the binder addition rate  $W_B$ . Formulation II and the single-dispersion mode of the binder were adopted. The  $D_{50}$  using the high speed mixer produced a large number of low  $W_B$ . High granular yields were obtained at  $W_B=9.1\%$  using the high speed mixer, and at  $W_B=10.3\%$  using the versatile mixer. These results imply a preference for the high speed mixer to increase the fine granule yields with a lower binder addition rate.

Figure 13 shows the shape index  $\psi_e$  for fine granules.  $\psi_e$  for 50 fine granules was measured and the mean was plotted. For  $\psi_e=1.0$  the granules were completely spherical. Spherical or semi-spherical fine granules were obtained using the versatile mixer.

The  $\psi_e$  using the high speed mixer was not always a large number because besides the spherical granules (Fig. 14a), egg-shaped granules (Fig. 14b) were generated. Figure 14 shows that the smooth surface is attributed to the agitator's vortex circulation and the chopper's shearing action. Well-compacted granules are obtained using formulation II with the high speed mixer.

### Conclusions

The following discoveries were made by investigating the granulation process and the granulation end-point of granules produced under different conditions. A high speed

mixer that automatically measured the power consumption and temperature, and a versatile mixer that continuously measured power consumption were employed.

(1) The granulation end-point that produced a high yield of spherical, well-compacted granules and fine granules was found in the area where a constant value of power consumption was indicated (initial stage of phase IV). This result was true regardless of the granulator model, formulation, or binder addition times. The temperature was one of the indicators of the granulation end-point.

(2) Regardless of the granulator model or formulation, the granulation process can be divided into four phases, with each phase demonstrating the same granulation mechanisms.

Phase I, formation of agglomerates and nucleic particle; phase II, growth into granular particles; phase III, granular refinement; phase IV, granulation completed.

(3) To compress the particle-size distribution and obtain high yields of fine granules, a longer binder addition period is preferred to a single dispersion because the nucleic particles developed into granules. The granulation process is categorized into four phases, regardless of the binder addition time.

(4) The high speed mixer offers better binder dispersion and shearing/compactness effects than the versatile mixer. Accordingly, the high speed device provides high yields of well-compacted granules and fine granules at a lower binder addition rate.

### References

- 1) K. Terashita, M. Yasumoto, and K. Miyamoto, *Yakugaku Zasshi*, **105**, 1166 (1985).
- 2) K. Terashita, M. Yasumoto, K. Miyamoto, and A. Ohike, *Yakugaku Zasshi*, **106**, 930 (1986).
- 3) K. Terashita, A. Ohike, M. Katou, and K. Miyamoto, *Yakugaku Zasshi*, **107**, 377 (1987).
- 4) P. Holm, T. Shaefer, and H. G. Kristensen, *Powder Tech.*, **43**, 213 (1985).
- 5) H. Leuenberger, *Manuf. Chem.*, **55**, 67 (1984); *idem, ibid.*, **55**, 53 (1984).
- 6) W. C. Fry, W. C. Stagner, and K. C. Wichman, *J. Pharm. Sci.*, **73**, 420 (1984).